HHS Public Access

Author manuscript

Ultrasound Med Biol. Author manuscript; available in PMC 2017 April 01.

Published in final edited form as:

Ultrasound Med Biol. 2016 April ; 42(4): 956–963. doi:10.1016/j.ultrasmedbio.2015.12.009.

Enhancement of Small Molecule Delivery by Pulsed-High Intensity Focused Ultrasound (pHIFU): A Parameter Exploration

Yufeng Zhou[1], **Yak-Nam Wang**[2], **Navid Farr**[3], **Jasmine Zia**[4], **Hong Chen**[5], **Bong Min Ko**[6], **Tatiana Khokhlova**[4], **Tong Li**[3], and **Joo Ha Hwang**[2,4]

[1]School of Mechanical and Aerospace Engineering, Nanyang Technological University, Singapore, 639798

[2]Center for Industrial and Medical Ultrasound, Applied Physics Laboratory, University of Washington, Seattle, WA, 98105

[3]Department of Bioengineering, University of Washington, Seattle, WA, 98105

[4]Division of Gastroenterology, School of Medicine, University of Washington, Seattle, WA, 98195

[5]Department of Biomedical Engineering, Washington University in St. Louis, St. Louis, MO, 63130

[6]Digestive Disease Center and Research Institute, Department of Internal Medicine, Soonchunhyang University College of Medicine, Korea

Abstract

Chemotherapeutic drug delivery is often ineffective within solid tumors, but increasing the drug dose would result in systemic toxicity. The use of high-intensity focused ultrasound (HIFU) has the potential to enhance penetration of **small molecules**. However, operation parameters need to be optimized before the use of chemotherapeutic drug *in vivo* and translation to clinical trial. In this study, the effects of pulsed-HIFU (pHIFU) parameters (spatial-average pulse-average intensity, duty factor, and pulse repetition frequency) to the penetration as well as **content** of small molecules were evaluated in *ex vivo* porcine kidneys. Specific HIFU parameters resulted in over 40 times greater Evans blue **content** and 3.5 times the penetration depth compared to untreated samples. When selected parameters were applied to porcine kidneys *in vivo*, a 2.3-fold increase in concentration was obtained after a 2-minute pHIFU exposure. Altogether, pHIFU has shown to be an effective modality to enhance both the concentration and penetration depth of **small molecules** into tissue using the optimized HIFU parameters. Although, performed in normal tissue, this study has the promise of translation into tumor tissue.

Corresponding Author: Dr. Yak-Nam Wang, Center for Industrial and Medical Ultrasound, Applied Physics Laboratory, University of Washington, 1013 Northeast 40th Street, Seattle, WA, 98105, USA, Tel: 206-616-6673, ynwang@u.washington.edu.

Keywords

pulsed-high intensity focused ultrasound (pHIFU); drug delivery; **content** and penetration; ultrasound parameters; kidney

Introduction

Globally, cancer accounts for nearly 1 in 8 deaths, more than HIV/AIDS, tuberculosis and malaria combined (Jemal et al. 2010). It is currently the second most common cause of death (behind cardiac disease) in the United States and countries of the European Union (Ferlay et al. 2010). According to surveillance, epidemiology, and end results (SEER) and mortality data from the National Center for Health Statistics (NCHS), it is estimated that within the US alone, approximately 1,658,370 new cancer cases diagnosed and about 589,430 cancer deaths in 2015 (American Cancer Society 2015).

Once diagnosed, there are numerous conventional and novel cancer therapies that are used, including surgery, radiotherapy, chemotherapy, immunotherapy, gene therapy, hyperthermia and phototherapy. However, all of these therapies have been slow if not ineffective in dramatically improving survival rates. Chemotherapeutics are often the treatment of choice, but conventional systemic administration results in saturation of normal tissue and non-selective cytotoxicity. In order for chemotherapeutics to be effective, there must be direct contact between the drug and the cancer cell with sufficient dose. However, increasing the drug dose would significantly increase the toxicity to healthy tissues. Although encapsulation of anti-cancer agents can mitigate the side effects accompanied by systemic delivery, a technique for controlled delivery is still required to release them to the cancerous tissue.

Efficacy and safety of cancer chemo- and bio-therapies are limited mainly due to poor penetration of anti-cancer drugs from the blood into tumor cells. The first barrier to overcome by the drug is the vessel wall. Solid tumors have a high vascular density but the blood vessels have anatomical and pathophysiological abnormalities, such as large gaps between endothelial cells. As a result, tumor tissues show selective extravasation and retention of macromolecular drugs, called the enhanced permeability and retention (EPR) effect (Fang et al. 2011). Once in the interstitium, molecule diffusion and convection can be slow due to high interstitial fluid pressure (IFP) as well as the presence of a prominent stromal matrix that separates the atypical vasculature from the tumor cells (Netti et al. 2000, Brown et al. 2003). Once at the cells, last physiological barrier for anti-cancer drugs is the cell membrane. There is a reservoir of clonogenic cells in the region between the maximum penetration of the drug and the onset of hypoxia, which can repopulate between sessions of chemotherapy. Therefore, strategies that enhance drug penetration have considerable potential to decrease cell viability. Anti-vascular endothelial growth factor treatment has been shown to render vessels more functional, resulting in a decrease in IFP and a subsequent improvement of drug diffusion within solid tumors (Jain 2005). The extracellular matrix can also be modified the enable drug penetration to distal cell layers by hyaluronidase treatment (Kerbel et al. 1996, St Croix et al. 1998) or pHIFU (Li et al. 2015).

Modification of the pH of acidic organelles can reduce the sequestering effect for more penetration of tumor tissue and toxic effects in the cell nucleus (Ouar et al. 2003).

The use of ultrasound energy to enhance efficiency of chemotherapy to tumors began as early as the 1970s (Frenkel 2008, Zhou 2013). The cytotoxic effect of nitrogen mustard on mouse leukemia L1210 cells after sonication without any mechanical damage to cells was observed (Kremkau et al. 1976). Tumors implanted into the hamster flank and sonicated with the co-administration of a chemotherapeutic (BCNU) improved the survival rate from 29.4% (sonication alone) to 40% (Fry and Johnson 1978).

Despite the promise of HIFU-enhanced drug delivery, the underlying mechanism is not fully understood and the parameters have yet to be optimized (Frenkel 2008, Mo et al. 2012). Most importantly, there are few studies on the role of HIFU on overcoming the interstitial barrier (Li et al. 2015). Current investigations are focused either on the transportation of the drug to the cancer cell through membrane or delivery to the xenografted tumor, which does not have the dense stromal structure as the naturally formed one (Primeau et al. 2005). The absence of a dense stromal matrix in the implanted tumor model may be the reason for discrepancies of the anti-cancer agent outcomes in animal experiments and clinical trials.

In this study, pHIFU was applied to enhance the penetration of small molecules into *ex vivo* tissue in order to explore a new strategy of overcoming the interstitial barrier. Both the mean arithmetic penetration depth and **content** of Evans blue albumin (EBA) were used to evaluate the **small molecule** delivery efficiency through the capsule of porcine kidney samples. Ultrasound parameters, spatial-average pulse-average acoustic intensity (I_{SAPA}), duty factor (*DF*), pulse repetition frequency (*PRF*), were varied to optimize the treatment conditions and investigate the underlying mechanism. Furthermore, the enhanced penetration and concentration of EBA to porcine kidneys after IV injection by pHIFU was also confirmed *in vivo*.

Materials and Methods

Experimental protocol

All experiments were performed with a custom-made air-backed concave HIFU transducer with a diameter of 34.9 mm, focal length of 50 mm, and resonant frequency of 1.16 MHz (Hwang et al. 2005). The driving electronics consisted of a function generator (33120A, Agilent Technologies, Palo Alto, CA, USA), an RF power amplifier (AP-400B, ENI, Rochester, NY, USA) and a custom-built impedance matching unit. A fiber optical probe hydrophone (FOPH-2000, RP Acoustics, Leutenbach, Germany) was mounted to a three-dimensional translation stage (minimum step size of 5 mm, BiSlide, Velmex, Bloomfield NY, USA), immersed in a testing tank filled with degassed water, and used to determine the characteristics of the transducer beam (-6 dB focal size of 4.1 mm ´× 12.6 mm, width×length). The acoustic power generated by the HIFU transducer was measured using a radiation force balance with an absorptive tile (Maruvada et al. 2007), and the spatial-average pulse-average acoustic intensity, I_{SAPA}, was calculated (Table 1) (Schafer and Lewin 1988). The acoustic parameters used in this study are listed in Table 2. A custom-built truncated cone was attached to the transducer and filled with degassed water to couple

the acoustic wave propagation. The tip of the cone (diameter 8 mm) was covered with a polyurethane membrane with an O-ring seal. A custom LabVIEW program (National Instrument, Austin, TX, USA) was used to control the sonication parameters (voltage amplitude of sinusoidal pulse, duty factor, burst duration and PRF).

Fresh porcine kidneys were obtained from an abattoir, carefully cut into blocks (25 × 25 × 37 mm), immersed in cold degassed phosphate buffered saline (PBS), and degassed for 60 minutes in a vacuum chamber. After degassing, each specimen was placed into custom-made sample holder (Fig. 1) with the fibrous capsule facing upwards. A custom-made cylindrical fluid holder was put in place (with a beveled edge being pushed into the tissue) to prevent leaking of the small-molecule solution (Evans blue dye bound to bovine serum albumin (BSA) and fluorescein sodium). Immediately prior to treatment, the remaining PBS within the fluid holder was aspirated and replaced with 1.5 ml of degassed solution of Evans blue dye (5 mg/ml), BSA (40 mg/ml), and fluorescein (1 mg/ml). The HIFU transducer was inserted into the fluid holder, and the top of *ex vivo* sample was aligned with the focal plane of the HIFU transducer by checking the time-of-flight (TOF) of the reflected signal using a pulser/receiver (PR7072R, Olympus IMS, Waltham, MA, USA) and a digital oscilloscope (Wavesurfer MXs-B, LeCroy, Chestnut Ridge, NY, USA). All samples were exposed to HIFU sonication for 2 minutes. For the control sample, the transducer was inserted into the fluid holder filled with EBA for 2 minutes without ultrasound exposure.

Quantitative analysis of drug delivery

Immediately following HIFU exposures or sham treatment, the samples were rinsed three times with PBS to remove surface bound Evans blue. The treated tissue was extracted using a 3 mm biopsy punch from the center of the *ex vivo* sample and then incubated in 500 μl formamide overnight to extract the EBA completely (Schumacher et al. 2006). The supernatant was removed from the tissue, and EBA concentration was determined from absorbance readings at 620 nm using a standard curve (Model 680, BioRad, Hercules, CA). Given the EBA is only in contact with the tissue at one surface, the concentration of EBA is dependent on the surface area of the tissue sampled rather than the weight of tissue. The final content of penetrating EBA is therefore expressed as total weight of EBA (mg) which was extracted from the sample.

For fluorescein penetration evaluation, samples were rinsed, bisected and embedded in optimum cutting temperature medium (O.C.T., TissueTek, Sakura, Alphen aan den Rij, the Netherlands) by immersing in isopentane cooled on dry ice. Three 10 μm sections were taken from the center of each sample and visualized on a digital fluorescence microscope (Eclipse 80i, Nikon Instrument, Melville, NY, USA) with a filter set of 470–490 nm for excitation and 520–560 nm for emission. Camera settings were kept constant for the photography of all samples. The maximum penetration depth was measured perpendicular to the sample surface using the intensity profile function in ImageJ software (National Institute of Health, Bethesda, MD, USA). Sustained intensity above the background value was taken to present fluorescein accumulation in the *ex vivo* samples. The mean arithmetic depths were calculated from the geometric depths to overcome any overestimation due to variations in the cutting angle (Wang et al. 2011). Samples that had significant erosion on the surface

were excluded in the sample analysis. Serial sections were also taken and stained with hematoxylin and eosin (H&E) for histological evaluation.

In vivo studies

The kidneys of two domestic swine were treated *in vivo* following a protocol approved by the Institutional Animal Care and Use Committee at the University of Washington. Animals were fasted for 24 h prior to the procedure with the exception of water. On the day of the procedure animals were sedated with an intramuscular (i.m.) injection of ketamine (22 mg/kg) and acetylpromazine (0.5–1.0 mg/kg) and intubated. Anesthesia was maintained using isofluorane (1.5%–2.5%) via endotracheal tube. The abdomen was opened, the intestines were moved to one side and overlying renal fascia was removed to reveal the kidney. The HIFU transducer with the coupling cone (same transducer used for the *ex vivo* studies) was coupled with the surface of the kidney, so the focal plane was about 1–2 mm below the surface. Ten minutes following Evans blue dye injection (50 mg/kg administered intravenously) the kidney was treated with pHIFU (I_{SAPA} = 900 W/cm^2, PRF = 10 Hz, 1% DF, 2 minutes). Five to six distinct locations were randomly selected in each of two kidneys per animal (2 animals). Each kidney had treated and sham regions. The exact treatment locations were marked immediately after sonication. Prior to euthanasia, the kidneys were perfused with phosphate buffered saline to wash out the residual EB. Samples from the treated and control regions were taken with a biopsy punch and weighed, and then incubated in formamide. The EB concentration was determined as for the *ex vivo* experiments and reported per weight of tissue. For the control sample, the HIFU transducer was placed on the porcine kidney for 2 minutes after IV injection of Evans blue but without HIFU exposure.

Statistical analysis

To determine differences in the measurements by condition, a one-way independent analysis of variance (ANOVA) was performed with *post hoc* tests. Significance was nominally set at $p < 0.01$. The p-statistic was adjusted depending on the number of comparisons (Bonferroni correction). The number of samples in each group varies from 3 to 22.

Results

After pHIFU exposure and rinsing the samples three times, blue circles could be observed clearly on the surface of the fibrous capsule (Fig. 2). At the same ultrasound intensity, the area and darkness of the blue circles appeared to depend on both DF and PRF. Because of a small tilting angle of the HIFU transducer in the experiment, the blue circle may shift slightly from the center of the fluid holder. Drug penetration (Fig. 3i) was measured from fluorescent imaging, and structural changes were qualitatively evaluated from the sequential sections stained with H&E (Fig. 3ii). In the control group, the penetration was less than 100 mm and only weak fluorescence was detected. After 2-min pHIFU sonication at I_{SAPA} = 940 W/cm^2, 4% DF and PRF of 1 Hz (40 ms pulse duration), there was a significant increase in penetration depth and intensity of the fluorescence observed at the center. Doubling the PRF at the same pulse duration (8% DF and PRF of 2 Hz) resulted in penetrations greater than 1 mm and a conical shape with a convergent angle similar to the focusing of our HIFU transducer. However, some erosion on the specimen surface, disrupted the hepatocellular

structure, and formation of cavities in the sonicated region were also found at these levels. Longer pulse durations (640 ms, 8% DF, and PRF of 0.125 Hz) also resulted in penetration depths greater than 1 mm, but caused severe disruption of the tissue. Tissue erosion is likely due to cavitation and occurred in the liquid despite degassing the EBA-fluorescein solution (Xu et al. 2004). This phenomenon occurred mostly with the longer burst duration and smaller PRF at the highest I_{SAPA} (i.e., I_{SAPA} = 940 W/cm^2, PRF = 0.1 Hz, DF = 8%, burst duration = 800 ms).

With varying the I_{SAPA} (705-940 W/cm^2, DF = 2%, PRF = 2 Hz), an increase in both mean EBA **content** and mean depth of penetration was observed in samples at intensities above 800 W/cm^2 (Fig. 4). At 940 W/cm^2, pHIFU results in about 3.5 times increase in penetration depth (908.0±283.9 μm vs. 256.3±99.8 μm) and 40 times increase in the tissue **content** of the EBA (8.34±4.44 μg vs. 0.20±0.28 μg) in comparison to the control. These increases were found to be significant at the p=0.001 level.

When the I_{SAPA} and burst duration were maintained at a constant value (940 W/cm^2, and 40 ms), the **content** of EBA and the depth of penetration showed an almost linear increase with an increasing DF (1–8 %) and PRF (0.25–2 Hz) (see Fig. 5). However, these increases were only significant ($p < 0.002$) above a DF of 2% (or 0.5 Hz PRF). Similar to increasing the intensity, trends in the depth of penetration matched that in the **content** of EBA extracted from the tissue.

In contrast, the trend became more complicated when changing the PRF from 0.125 Hz to 20 Hz or the pulse duration from 640 ms to 4 ms but maintaining the I_{SAPA} and duty factor at a constant value (940 W/cm^2 and 8%, respectively, in Fig. 6). Both the depth of penetration and EBA **content** displayed a peak at PRF of 0.125 Hz (12.76±5.85 μg and 820.1±230.1 μm) and 2 Hz (8.37±4.44 μg and 907.98±283.92 μm) or a pulse duration of 40 ms and 640 ms, both of which were significantly greater than the control ($p < 0.001$).

In vivo experiments also confirmed the enhancement in **small molecule** delivery by pHIFU (see Fig. 7). There is a 2.3-fold increase of EBA concentration per weight in the porcine kidney (from 11.4±2.9 ng/mg to 25.9±13.9 ng/mg). Although the standard deviation is large, which may be due to absence of imaging guidance and the heterogeneity of tissue, the difference between the test groups is significant ($p < 0.002$).

Discussion

In this study, pHIFU was utilized to enhance **small molecule** penetration. A frequency of 1.1 MHz was selected as a tradeoff between the maximum propagation distance of ultrasound and the focused beam width to target an abdominal organ, which is similar to the driving frequencies of most clinical extracorporeal HIFU devices in the tumor ablation (Illing et al. 2005, Xiong et al. 2009). The effects of HIFU parameters to the penetration depth as well as the **content** of small molecule agents have been evaluated using an *ex vivo* model. Both the penetration depth and EBA **content** was found to increase with I_{SAPA}, pulse duration, and duty factor. At 940 W/cm^2, pHIFU results in about 3.5 times increase in penetration depth and 40 times increase in the tissue **content** of the EBA compared to the

control. The higher standard deviation at high intensities (i.e., 870 and 940 W/cm^2) may be due to the variation of kidney samples, random formation of internal cavities and tissue disruption as seen in Fig. 3ii. The higher intensities can also result in a greater likelihood of cavitation which has been shown to result in increase in drug delivery (Li et al. 2015).

The relationship to the PRF or pulse duration was found to be bi-modal; a double peak in both depth of penetration and EBA **content** was present. This double-peak structure could be due to different effects of the pulse duration and PRF on the drug penetration and **content** and increasing PRF while decreasing pulse duration in order to keep the same duty cycle or effective exposure time (HIFU activation time). Such a biomodal relationship suggests that the effective exposure time is not the deterministic parameter of **small molecule** delivery.

Evans blue dye and sodium fluorescein were chosen due to their molecular weights being within the range of common chemotherapeutic agents. Kidney specimens were used because the fibrous capsule simulated the fibrous stroma that is seen in tumors (Olive et al. 2009). The key to successful treatment of tumors resides in more effective penetration of sufficient amounts of chemotherapeutics without causing significant toxicity to normal tissues. It has been demonstrated that the concentration of chemotherapeutic agent administered intravenously decreases exponentially with distance from the tumor blood vessels and with the characteristic penetration distance of about 40–50 μm, representing the distance from the nearest vessel where the concentration decreases to half of the perivascular value. However, the mean distance from blood vessels to regions of hypoxia was 90–140 μm (Primeau et al. 2005). Therefore, greater penetration of systemically administered chemotherapeutic agents is needed to reach viable malignant cells. The penetration depth produced by pHIFU in our study is approximately 6 times greater than this distance, suggesting that the interstitial barrier could be overcome by this method. Furthermore, our preliminary *in vivo* study confirmed the *ex vivo* penetration of enhanced EB penetration and concentration by pHIFU and establish the foundation for the future experiments of tumor drug delivery. Indeed, pHIFU has been shown to increase the concentration of doxorubicin to tumors with high stromal content by up to 4.5 fold (Li et al. 2015).

Pulsed-HIFU has the potential for enhancing the penetration of various agents with different formulations (small molecules, DNA, and nanoparticles) in solid tumors (Frenkel 2008, Mo et al. 2012, Li et al. 2015). It has the advantages of immediate enhancement without pre-treatment; no modification to the chemotherapeutic agent; the ability to target tumors without damaging intervening tissue; and theoretically, an unlimited number of treatment sessions. With changes only to the operation parameters, clinical HIFU systems can be used in conjunction with chemotherapy. Initial trials of HIFU ablation of unresectable pancreatic cancer during chemotherapy showed higher survival and longer time to tumor progression than chemotherapy alone (19.5 vs. 10.3 months and 11.6 vs. 4.4 months respectively). No major complications were reported (Lee et al. 2011). Our study suggests that such enhanced drug delivery depends on the HIFU parameters used. Parameter optimization is necessary to achieve the best clinical outcome and may be repeated for different targets because of their physiological properties and anatomical characteristics.

The thermal effect is negligible in pHIFU because of the low duty factor, and no coagulative necrosis was observed from our histological evaluation. This suggests that the underlying mechanism is mostly mechanical, such as bubble cavitation, acoustic radiation force and associated streaming. Increasing the efficiency of drug penetration in solid tumors in pHIFU treatment should be based on the further understanding of the dominant mechanism.

There are a few limitations of this study. First, porcine kidney samples were used to prove the concept of enhancing drug penetration with pHIFU and considered the most ideal tissue after testing multiple different tissues, including liver, muscle, and gastrointestinal epithelium because their fibrous capsule best simulated the fibrous stroma as seen in tumors. But this model cannot completely simulate all physiological barriers and vasculature properties in chemotherapeutic drug delivery. Transgenic animal model with naturally grown tumor instead of xenograft models should be used later to confirm the outcome, quantitative drug penetration and concentration in the acute study. Although Evans blue has been used widely as drug surrogate in the cancer chemotherapy investigation because of easy observation and quantification by spectrophotometry (Matsumura and Maeda 1986), tumor regression in the survival study using chemotherapeutic agent is necessary to evaluate the therapeutic potential. Second, although bubble cavitation is assumed as an important mechanism, its dose in the experiment was not measured. By using a passive acoustic sensor tuned to higher frequencies and aligned confocally with the HIFU transducer, cavitation noise emanating from the HIFU focus could be monitored noninvasively (Coussios and Roy 2008). Stable and inertial bubble cavitation produce subharmonics of driving frequency and broadband white noise, respectively. Thus, they can be delineated using spectrum analysis (i.e., small-time Fourier transform) and monitored continuously during treatment. Cavitation monitoring would allow further understanding of the role and variation of cavitation in the drug delivery. Third, there was no real-time imaging used to monitor the progress of drug delivery. Measuring drug pharmacokinetics and physiological parameters simultaneously and continuously with high spatial and temporal resolution is important in investigating the role of each physiological barrier, but is extremely challenging (Jain 1999).

In conclusion, pHIFU has the ability improve the penetration depth and concentration of small molecules into tissue. Its performance is dependent on the ultrasound parameters selected. Thus, parameter exploration and optimization are important for application. Preliminary *in vivo* experiments confirm the enhanced delivery of IV injected EBA to porcine kidney. Future *in vivo* studies are required to further evaluate the potential of this technology for clinical transition.

Acknowledgments

This work was supported by NIH grants 1R01CA154451, 5R03DK084126-02 and the Washington State Life Science Discovery Fund.

References

American Cancer Society. Cancer Facts and Figures 2015. 2015.

Brown E, McKee T, diTomaso E, Pluen A, Seed B, Boucher Y, Jain RK. Dynamic imaging of collagen and its modulation in tumors in vivo using second-harmonic generation. Nat Med. 2003; 9:796–800. [PubMed: 12754503]

Coussios CC, Roy RA. Applications of acoustics and cavitation to noninvasive therapy and drug delivery. Annu Rev Fluid Mech. 2008; 40:35–420.

Fang J, Nakamura H, Maeda H. The EPR effect: unique features of tumor blood vessels for drug delivery, factors involved, and limitations and augmentation of the effect. Advanced Drug Delivery Reviews. 2011; 63:136–151. [PubMed: 20441782]

Ferlay J, Parkin DM, Steliarova-Foucher E. Estimates of cancer incidence and mortality in Europe in 2008. Eur J Cancer. 2010; 46:765–781. [PubMed: 20116997]

Frenkel V. Ultrasound mediated delivery of drugs and genes to solid tumors. Advanced Drug Delivery Reviews. 2008; 60:1193–1208. [PubMed: 18474406]

Fry FJ, Johnson LK. Tumor irradiation with intense ultrasound. Ultrasound Med Biol. 1978; 4(4):337–341. [PubMed: 753007]

Hwang JH, Brayman AA, Reidy MA, Matula TJ, Kimmey MB, Crum LA. Vascular effects induced by combined 1-MHz ultrasound and microbubble contrast agent treatments in vivo. Ultrasound Med Biol. 2005; 31(4):553–564. [PubMed: 15831334]

Illing RO, Kennedy JE, Wu F, ter Haar GR, Protheroe AS, Friend PJ, Gleeson FV, Cranston DW, Phillips RR, Middleton MR. The safety and feasibility of extracorporeal high-intensity focused ultrasound (HIFU) for the treatment of liver and kidney tumours in a Western population. British Journal of Cancer. 2005; 93:890–895. [PubMed: 16189519]

Jain RK. Understanding barriers to drug delivery: high resolution *in vivo* imaging is key. Clin Cancer Res. 1999; 5:1605. [PubMed: 10430057]

Jain RK. Normalization of tumor vasculature: an emerging concept in antiangiogenic therapy. Science. 2005; 307:58–62. [PubMed: 15637262]

Jemal A, Siegel R, Xu J, Ward E. Cancer statistics. Cancer J Clin. 2010; 60:277–300.

Kerbel RS, St Croix B, Florenes VA, Rak J. Induction and reversal of cell adhesion-dependent multicellular drug resistance in solid breast tumors. Hum Cell. 1996; 9:257–264. [PubMed: 9183656]

Kremkau FW, Kaufmann JS, Walke MM, Burch PG, Spurr CL. Ultrasonic enhancement of nitrogen mustard cytotoxicity in mouse leukemia. Cancer. 1976; 37:1643–1647. [PubMed: 1260681]

Lee JY, Choi BI, Ryu JK, Kim YT, Hwang JH, Kim SH, Han JK. Concurrent chemotherapy and pulsed high-intensity focused ultrasound therapy for the treatment of unresectable pancreatic cancer: initial experiences. Korean J Radiol. 2011; 12:176–186. [PubMed: 21430934]

Li T, Wang YN, Khokhlova TD, D'Andrea S, Starr F, Chen H, McCune JS, Risler LJ, Mashadi-Hossein A, Hwang JH. Pulsed high intensity focused ultrasound (pHIFU) enhances delivery of doxorubicin in a preclinical model of pancreatic cancer. Cancer Res. 2015 epub.

Maruvada S, Harris GR, Herman BA, King RL. Acoustic power calibration of high-intensity focused ultrasound transducers using a radiation force technique. J Acous Soc Am. 2007; 121:1434–1439.

Matsumura Y, Maeda H. A new concept for macromolecular therapeutics in cancer chemotherapy: mechanism of tumoritropic accumulation of proteins and the antitumor agent smancs. Cancer research. 1986; 46:6387–6392. [PubMed: 2946403]

Mo S, Coussios CC, Seymour L, Carlisle R. Ultrasound-enhanced drug delivery for cancer. Expert Opinion on Drug Delivery. 2012; 9:1525–1538. [PubMed: 23121385]

Netti PA, Berk DA, Swartz MA, Grodzinsky AJ, Jain RK. Role of extracellular matrix assembly in interstitial transport in solid tumors. Cancer Res. 2000; 60:2497–2503. [PubMed: 10811131]

Olive KP, Jacobetz MA, Davidson CJ, Gopinathan A, Mclntyre D, Honess D, Madhu B, Goldraben MA, Caldwell ME, Allard D, Frese KK, DeNicola G, Feig C, Combs C, Winter SP, Ireland-Zecchini H, Reichelt S, Howat WJ, Chang A, Dhara M, Wang L, Rückert F, Grützmann R, Pilarsky C, Izeradjene K, Hingorani SR, Huang P, Davies SE, Plunkett W, Egorin M, Hruban RH, Whitebread N, McGovern K, Adams J, Iacobuzio-Donahue Christine, Griffiths J, Tuveson DA. Inhibition of hedgehog signaling enhances delivery of chemotherapy in a mouse model of pancreatic cancer. Science. 2009; 324:1457–1461. [PubMed: 19460966]

Ouar Z, Bens M, Vignes C, Paulais M, Pringel C, Fleury J, LCluzeaud F, Lacave R, Vandewalle A. Inhibitors of vacuolar H+-ATPase impair the preferential accumulation of daunomycin in lysosomes and reverse the resistance to anthracyclines in drug-resistant renal epithelial cells. Biochem J. 2003; 370:185–193. [PubMed: 12435274]

Primeau AJ, Rendon A, Hedley D, Lilge L, Tannock IF. The distribution of the anticancer drug doxorubicin in relation to blood vessels in solid tumors. Clinical Cancer Research. 2005; 11:8782–8788. [PubMed: 16361566]

Schafer ME, Lewin PA. A computerized system for measuring the acoustic output from diagnostic ultrasound equippment. IEEE transactions on Ultrasonics, Ferroelectrics, and Frequency Control. 1988; 35:102–109.

Schumacher J, Puchakayala MR, Binkowski K, Eichler W, Dendorfer A, Klotz KF. Effects of candesartan and enalaprilat on the organ-specific microvascular permeability during haemorrhagic shock in rats. Br J Anaesth. 2006; 96(4):437–443. [PubMed: 16490762]

St Croix B, Man S, Kerbel RS. Reversal of intrinsic and acquired forms of drug resistance by hyaluronidase treatment of solid tumors. Cancer Letters. 1998; 131:35–44. [PubMed: 9839618]

Wang YN, Lee K, Ledoux WR. Histomorphological evaluation of diabetic and non-diabetic plantar soft tissue. Foot Ankle Int. 2011; 32(8):802–810. [PubMed: 22049867]

Xiong LL, Hwang JH, Huang XB, Yao SS, He CJ, Ge XH, Ge HY, Wang XF. Early clinical experience using high intensity focused ultrasound for palliation of inoperable pancreatic cancer. Journal of Pancreas. 2009; 10:123–129.

Xu Z, Ludomirsky A, Eun LY, Hall TL, Tran BC, Fowlkes JB, Cain CA. Controlled ultrasound tissue erosion. IEEE transactions on Ultrasonics, Ferroelectrics, and Frequency Control. 2004; 51:726–36.

Zhou YF. Ultrasound-mediated drug/gene delivery in solid tumor treatment. Journal of Healthcare Engineering. 2013; 4:223–254. [PubMed: 23778013]

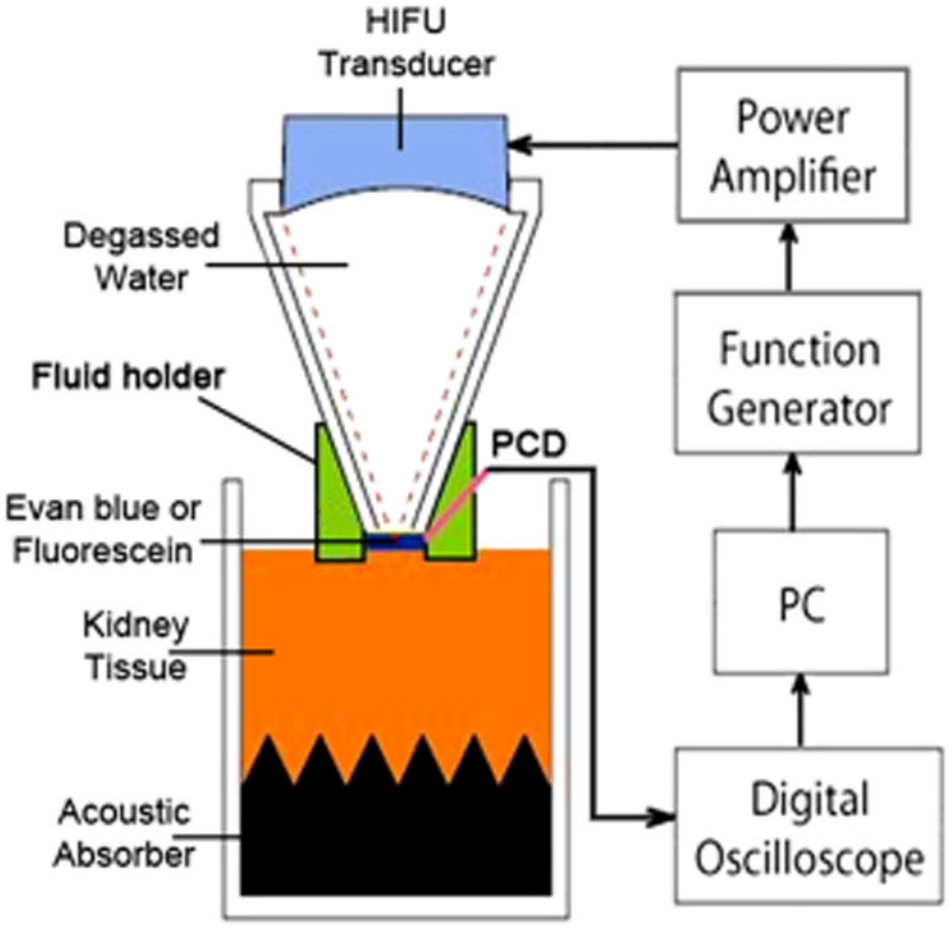

Figure 1.
Schematic of the experimental setup. Degassed kidney samples were placed in a custom holder with an acoustic absorber at the bottom. A custom-built fluid holder was placed on top of the kidney tissue.

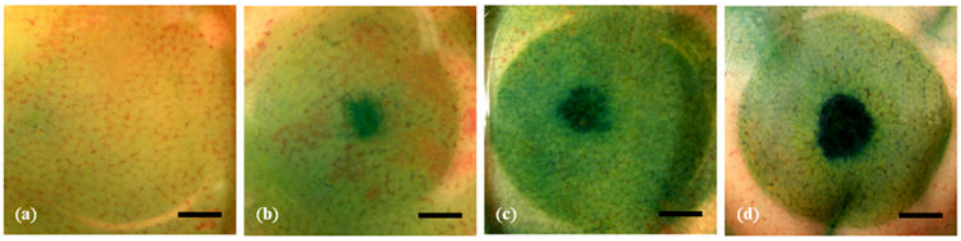

Figure 2.

Representative photos of the rinsed surface of the kidneys after sonication. The control samples (a) exhibited a homogenous light blue hue. Blue circles could be observed in the tissue after 2-min pulsed-HIFU exposure of (b) 940 W/cm^2, 4% DF, 1 Hz PRF, (c) 940 W/cm^2, 8% DF, 2 Hz PRF, and (d) 940 W/cm^2, 8% DF, 0.125 Hz PRF. Scale bar represents 3 mm. DF: duty factor; PRF: pulse repetition frequency.

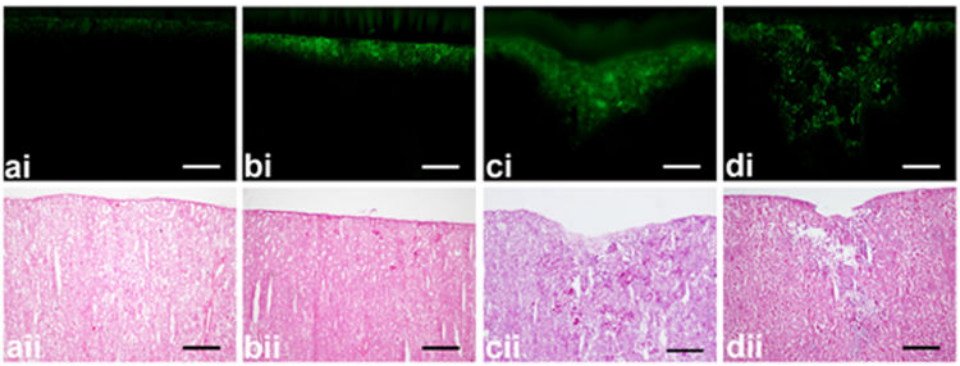

Figure 3.

Representative (i) fluorescent images and (ii) Hematoxylin and Eosin stained sections after (a) control and 2-min pulsed-HIFU exposure of (b) 940 W/cm^2, 4% DF, 1 Hz PRF, (c) 940 W/cm^2, 8% DF, 2 Hz PRF, and (d) 940 W/cm^2, 8% DF, 0.125 Hz PRF. Control samples showed an even layer of fluorescence compared to the sonicated samples which often exhibited an area of fluorescence in the shape of a cone. Tissue erosion on the sample surface is evident in both the fluorescent images (di) and after staining with H&E (dii). Scale bar represents 500 μm. DF: duty factor; PRF: pulse repetition frequency.

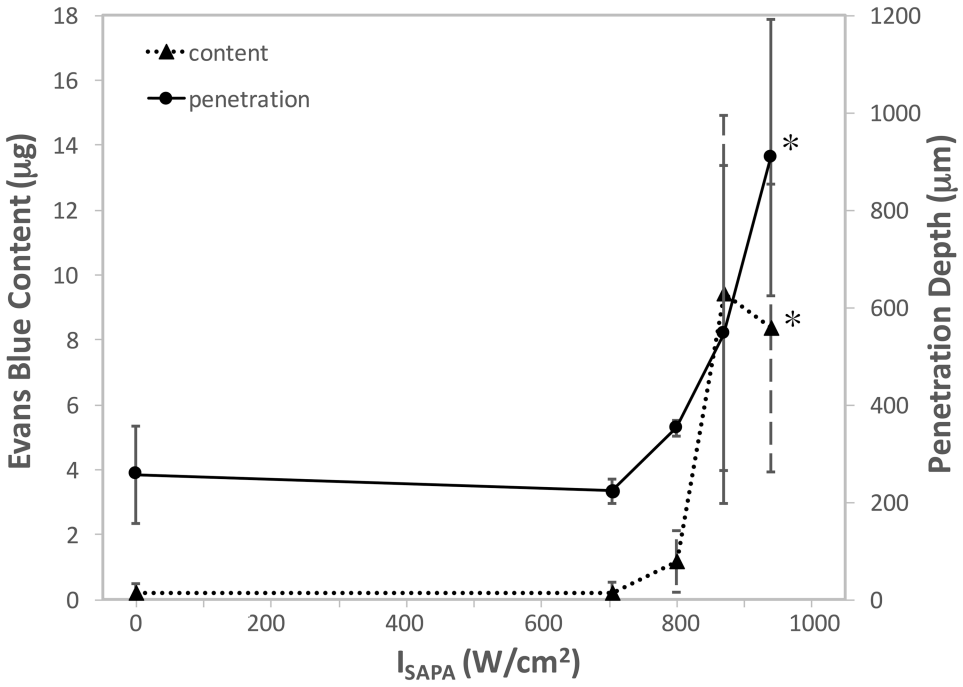

Figure 4.

Mean Evans blue albumin (EBA) content (triangle; dotted line) and mean arithmetic penetration depth (circle; solid line) in samples treated with varying spatial-average pulse-average acoustic intensity (I_{SAPA} = 705-940 W/cm^2), whilst keeping the duty factor, pulse repetition frequency, and pulse duration constant (8%, 2 Hz, and 40 ms, respectively). Error bars represent standard deviation. *: statistically different in comparison to the control.

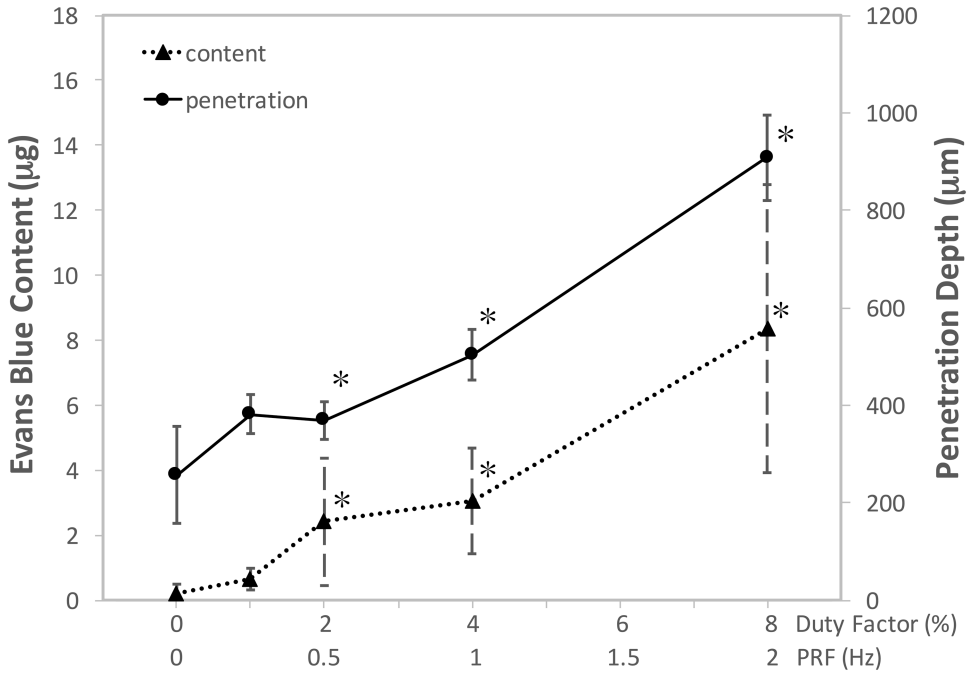

Figure 5.

Mean Evans blue albumin (EBA) content (triangle; dotted line) and mean arithmetic penetration depth (circle; solid line) in samples treated with varying duty factor (1-8 %) and pulse repetition frequency (0.25-2 Hz), whilst keeping the spatial-average pulse-average acoustic intensity and pulse duration constant (940 W/cm^2 and 40 ms). Error bars represent standard deviation. *: statistically different in comparison to the control.

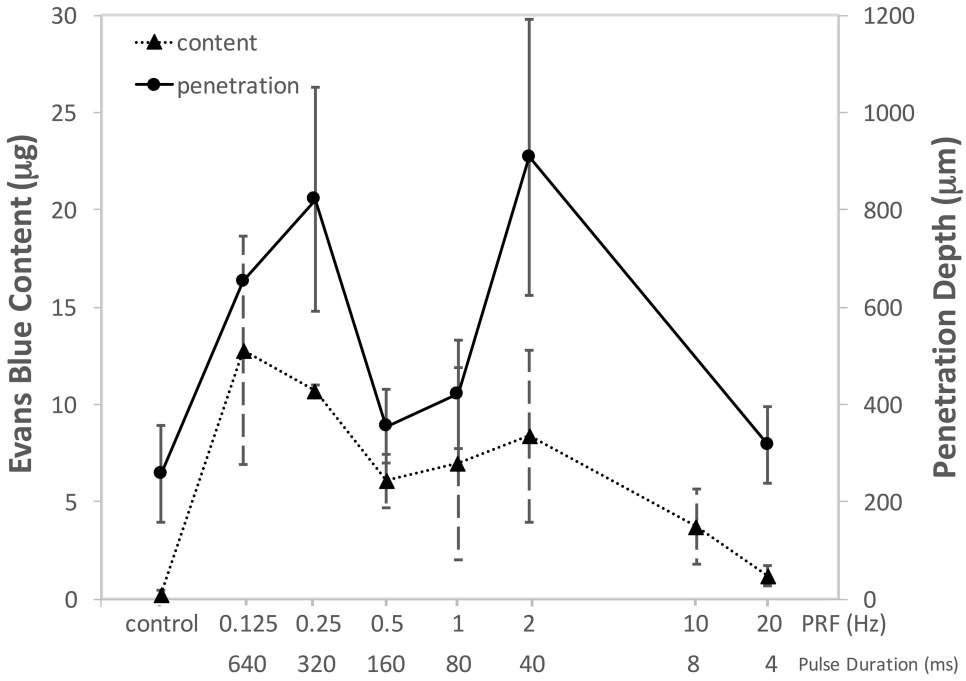

Figure 6.

Mean Evans blue albumin (EBA) content (triangle; dotted line) and mean arithmetic penetration depth (circle; solid line) in samples treated with varying pulse repetition frequencies (PRF) and pulse duration, whilst keeping the duty factor and spatial-average pulse-average acoustic intensity constant (DF = 8% and I_{SAPA} = 940 W/cm^2). Error bars represent standard deviation.

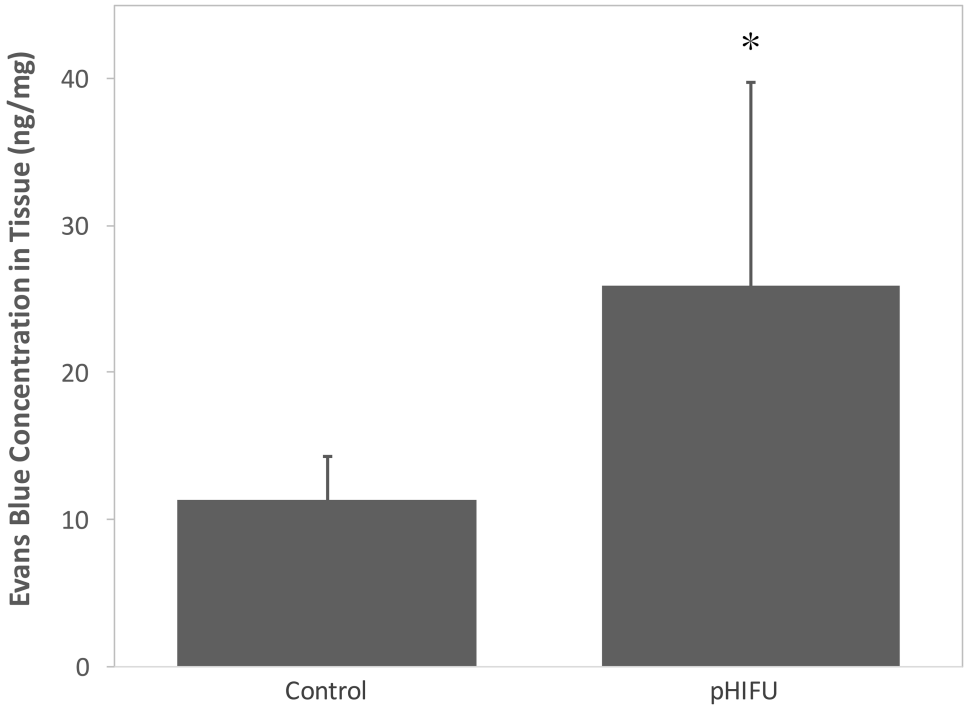

Figure 7.

Comparison of mean Evans blue albumin (EBA) concentration in the porcine kidney *in vivo* (I_{SAPA} = 900 W/cm^2, PRF = 10 Hz, 1% DF). Error bars represent standard deviation. *: statistically different in comparison to the control.

Table 1

Measured peak positive and peak negative pressure at the focus and spatial-average pulse-average acoustic intensity of the HIFU transducer at varying output levels.

I_{SAPA} (W/cm^2)	$\lvert p^- \rvert$ (MPa)	p^+ (MPa)
705	3.68	10.72
800	4.21	13.21
870	5.96	16.89
940	6.79	19.23

Table 2

Summary of HIFU parameters used in both *ex vivo* and *in vivo* studies.

	I_{SAPA} (W/cm^2)	PRF (Hz)	Pulse duration (ms)	Duty factor (%)	Number of samples
ex vivo	0 (control)	0	0	0	21
	705	2	40	8	5
	800	2	40	8	5
	870	2	40	8	5
	940	2	40	8	12
	940	0.25	40	1	5
	940	0.5	40	2	3
	940	1	40	4	5
	940	0.125	640	8	3
	940	0.25	320	8	4
	940	0.5	160	8	3
	940	1	80	8	3
	940	10	8	8	4
	940	20	4	8	5
in vivo	0 (control)	0	0	0	11
	900	10	1	1	11